A&A 375, 899–908 (2001)
DOI: 10.1051/0004-6361:20010886

Astronomy & Astrophysics

Light element non-LTE abundances of λ Bootis stars

II. Nitrogen and sulphur⋆

I. Kamp[1], I. Kh. Iliev[2], E. Paunzen[3,4], O. I. Pintado[5,7], E. Solano[6,7], and I. S. Barzova[2]

[1] Leiden Observatory, Niels Bohrweg 2, PO Box 9513, 2300 RA Leiden, The Netherlands
[2] Institute of Astronomy, National Astronomical Observatory, and Isaac Newton Institute of Chile Bulgarian Branch, PO Box 136, 4700 Smolyan, Bulgaria
e-mail: rozhen@mbox.digsys.bg
[3] Institut für Astronomie der Universität Wien, Türkenschanzstr. 17, 1180 Wien, Austria
e-mail: Ernst.Paunzen@univie.ac.at
[4] Zentraler Informatikdienst der Universität Wien, Universitätsstr. 7, 1010 Wien, Austria
[5] Departamento de Física, Facultad de Ciencias Exactas y Tecnología, Universidad Nacional de Tucumán, Argentina – Consejo Nacional de Investigaciones Científicas y Técnicas de la República Argentina, Argentina
e-mail: opintado@tucbbs.com.ar
[6] Laboratorio de Astrofísica Espacial y Física Fundamental (LAEFF), Apartado de Correos 50727, 28080 Madrid, Spain
e-mail: esm@vilspa.esa.es
[7] Visiting Astronomers at Complejo Astronomico El Leoncito

Received 18 May 2001 / Accepted 31 May 2001

Abstract. One of the main characteristics proclaimed for the group of the λ Bootis stars is the apparent solar abundance of the light elements C, N, O and S. The typical abundance pattern is completed by the strong underabundances of the Fe-peak elements. In the first paper of this series, we have shown that carbon is less abundant than oxygen but both elements are still significantly more abundant than Fe-peak elements. The mean abundances, based on a detailed non-LTE investigation, were found −0.37 dex and −0.07 dex, respectively. As a further step, we now present non-LTE abundances of nitrogen and sulphur for thirteen members of the λ Bootis group based on several spectral lines between 8590 Å and 8750 Å. Furthermore, LTE abundances for calcium in the same spectral range were derived and compared with values from the literature. Similar to the mean abundances of carbon and oxygen, nearly solar values were found (−0.30 dex for nitrogen and −0.11 dex for sulphur) for our sample of program stars. Among our sample, one previously undetected binary system (HD 64491) was identified. From a statistical point of view, the abundances of the light elements range from slightly overabundant to moderately underabundant compared to the Sun. However, the individual objects always exhibit a similiar pattern, with the Fe-peak elements being significantly more underabundant than the light elements. No correlation of the derived abundances with astrophysical parameters such as the effective temperature, surface gravity or projected rotational velocity was found. Furthermore, the abundances of the light elements do not allow us to discriminate between any proposed theory.

Key words. stars: abundances – stars: atmospheres – stars: chemically peculiar – stars: early-type

1. Introduction

The λ Bootis stars are late B to early F-type dwarfs whose atmospheres show moderate to strong metal deficiencies of heavy elements like iron, calcium, and magnesium. They cover an area slightly above the main sequence in the Hertzsprung-Russell-diagram (Paunzen 1997). In the literature there is still a debate on the nature and evolutionary state of these stars.

Send offprint requests to: I. Kamp,
e-mail: kamp@strw.leidenuniv.nl

⋆ Based on observations obtained at BNAO Rozhen and Complejo Astronómico el Leoncito (CASLEO), operated under the agreement between the Consejo Nacional de Investigaciones Científicas y Técnicas de la República Argentina and the National Universities of La Plata, Córdoba y San Juan.

Some of the brightest λ Bootis stars which were observable by IRAS are known to have an infrared excess (Aumann et al. 1984; Sadakane & Nishida 1986; Gillett 1986; Gerbaldi 1991; Cheng et al. 1992; Oudmaijer et al. 1992; Waters et al. 1992). Holweger & Rentzsch-Holm (1995) and Holweger et al. (1999) find that about 30% of a sample of 18 λ Bootis stars show narrow circumstellar absorption lines in Ca II K. The correlation between the presence of these features and the rotational velocity suggests that these lines arise in equatorial disks surrounding the rotating λ Bootis stars.

The abundance pattern of the λ Bootis stars resemble very much the pattern found for evolved AGB stars: C, N, O and S show approximately solar abundances while all other metals are depleted by up to 3 orders of magnitude (Venn & Lambert 1990; Heiter 2000). These evolved stars are surrounded by shells which are the result of the mass-loss phase on the AGB. Their peculiar abundance pattern might be linked to the existence of shells around them. Hence a possible scenario to explain the strange abundance pattern of λ Bootis stars is the selective accretion of circumstellar gas depleted in condensable elements.

Michaud & Charland (1986) and Charbonneau (1993) worked out a diffusion/mass-loss scenario, which can explain the underabundances of heavy elements by an interplay between gravitational settling and radiative levitation of an element in the presence of a small mass-loss rate of typically 10^{-13} $M_\odot$ yr^{-1}. Unfortunately, meridional circulation efficiently counteracts this separation process, even at moderate rotational velocities.

Facing these difficulties, Charbonneau (1991) and Turcotte & Charbonneau (1993) came up with an accretion/diffusion scenario, where metal-depleted material from the interstellar medium is accreted onto the star at rates larger than 10^{-14} $M_\odot$ yr^{-1}. The critical point is again mixing by meridional circulation especially after the accretion has ceased.

Andrievsky (1997) postulated that some λ Bootis stars are mergers from W UMa type binary systems. This scenario nicely explains the presence of circumstellar material and leads to a peculiar abundance pattern in the stellar atmosphere due to nuclear processed material.

Faraggiana & Bonifacio (1999) showed that a general metal-deficiency may be mimiked by the composition of two spectra with solar abundances but different effective temperatures, $\log g$ and $v \sin i$.

A still unresolved question is the evolutionary state of these stars. Several facts point towards an explanation of the λ Bootis phenomenon in terms of a pre-main-sequence evolutionary phase:

- the discovery of λ Bootis stars in the Orion OB1 association, in the young open cluster NGC 2264 and among pre-main-sequence Ae stars (Gray & Corbally 1993; Gray & Corbally 1997);
- the high incidence of circumstellar gas and the preference of rapid rotation for λ Bootis stars (Holweger & Rentzsch-Holm 1995; Holweger et al. 1999);
- on the basis of the new Hipparcos data the λ Bootis stars lie very close to and above the main-sequence (Paunzen 1997).

This short overview reveals that there is a variety of ideas to explain the existence of λ Bootis stars. There is definitely a need to have a homogeneous set of surface abundances for a sample of these stars, in order to be able to discriminate between some of the proposed scenarios.

In a first paper, Paunzen et al. (1999b, hereafter Paper I) determined the NLTE abundances of C and O in a large sample of λ Bootis stars. They found that the strong anticorrelation first noted by Holweger & Stürenburg (1993) is clearly present. The refractory elements Fe and Si are condensed in the dust phase of the circumstellar material, while the volatile elements C, N, O and S remain in the gas phase. This anticorrelation hints at an explanation of the abundance pattern in the framework of an accretion scenario. Following the work of Rentzsch-Holm (1997) we derive now for a sample of λ Bootis stars NLTE N and S abundances from the 8700 Å region.

2. Program stars and observation

Stars from the target list have been observed with the coudé spectrograph at the 2 m RCC telescope of the Bulgarian National Astronomical Observatory Rozhen (see Table 1). Spectra have been recorded with a Photometrics AT200 camera (SITe SI003AB 1024 × 1024 CCD chip) using a 632 mm^{-1} Baush & Lomb grating in the first order and the Third camera of the spectrograph. The spectral region was centered on 8670 Å. As a result the resolution reached in a 200 Å large frame is about 22 000. A hollow-cathode FeAr lamp (ThAr since January 2000) was used to produce a spectrum with a FWHM of about 2 pixels for the reference lines. A tungsten projection lamp mounted in front of the entrance slit of the spectrograph was used for retrieving flat fields.

Table 1. Observing log of program stars.

HD	HR	Name	V	Date	Telescope
31295	1570	π^1 Ori	4.64	09.11.1998	BNAO
64491	3083	DD Lyn	6.23	10.11.1998	BNAO
				06.11.2000	BNAO
75654	3517	HZ Vel	6.38	11.05.1998	CASLEO
91130	4124	33 LMi	5.93	10.11.1998	BNAO
111005			7.95	12.05.1998	CASLEO
120500		FQ Boo	6.61	29.12.1998	BNAO
125162	5351	λ Boo	4.18	29.12.1998	BNAO
141851	5895		5.10	27.02.1999	BNAO
142703	5930	HR Lib	6.12	27.02.1999	BNAO
148638			7.90	11.05.1998	CASLEO
149303	6162		5.77	30.12.1998	BNAO
183324	7400	35 Aql	5.77	27.02.1999	BNAO
192640	7736	29 Cyg	4.95	06.11.2000	BNAO
193281	7764A		6.61	11.05.1998	CASLEO
204041	8203		6.45	05.10.1998	BNAO
221756	8947	15 And	5.59	09.11.1998	BNAO

Table 2. Line list and atomic parameters for the spectrum synthesis; the columns indicate the ionization state, the wavelength, the excitation potential of the lower level, the oscillator strength (N: Wiese et al. 1996; Al, Ca: Wiese et al. 1966; Mg, Si, S, Fe: Kurucz 1993), van der Waals broadening (approximation of Unsöld 1968), Stark broadening (for ions: Griem 1968; for neutrals: Cowley 1971), and radiative damping (classical formula). The last two columns denote the lower and upper level numbers of the respective nitrogen model atom (Rentzsch-Holm 1996). The hydrogen lines are calculated using the broadening tables of Lemke (1997).

Element	Wavelength [Å]	χ_i [eV]	$\log gf$	$\log C_4$	$\log C_6$	$\log \gamma_{rad}$ [10^8 s^{-1}]	i	j
N I	8594.00	10.67	−0.334	−29.86	−13.02	0.30	5	12
Si I	8595.96	6.19	−1.040	−28.25	−10.96	0.30		
H I	8598.39							
Fe I	8598.83	4.39	−1.089	−29.58	−12.82	0.30		
Fe I	8611.80	2.85	−1.926	−30.90	−13.55	0.30		
Fe I	8616.28	4.91	−0.405	−29.37	−12.43	0.30		
S I	8617.09	8.41	−0.410	−29.82	−10.94	0.30		
S I	8626.54	8.41	−0.540	−29.82	−10.94	0.30		
N I	8629.24	10.69	+0.075	−29.86	−13.02	0.30	5	12
S I	8633.12	8.41	−0.060	−29.83	−10.94	0.30		
Al II	8640.70	11.82	−0.018	−30.20	−12.78	0.30		
Si I	8648.47	6.21	−0.300	−28.22	−10.93	0.30		
S I	8655.17	8.41	−0.540	−29.83	−10.95	0.30		
N I	8655.88	10.69	−0.627	−29.86	−13.02	0.30	5	12
Fe I	8661.90	2.22	−1.537	−30.46	−13.76	0.30		
Ca II	8662.14	1.69	−0.620	−30.24	−13.38	0.30		
H I	8665.02							
S I	8668.44	8.41	+0.210	−29.83	−10.96	0.30		
S I	8670.19	7.87	−0.890	−28.97	−11.93	0.30		
S I	8670.65	7.87	−0.530	−28.97	−11.93	0.30		
S I	8671.37	7.87	−0.640	−28.97	−11.93	0.30		
Fe II	8671.88	6.14	−2.788	−30.72	−13.35	0.30		
Fe I	8674.75	2.83	−1.800	−30.92	−13.56	0.30		
S I	8679.00	7.87	−1.000	−28.97	−11.93	0.29		
S I	8679.70	7.87	−0.410	−28.97	−11.93	0.29		
Si I	8680.08	5.86	−1.000	−28.73	−11.65	0.29		
N I	8680.28	10.34	+0.346	−30.06	−13.20	0.29	4	8
S I	8680.47	7.87	−0.230	−28.97	−11.93	0.29		
N I	8683.40	10.33	+0.086	−30.07	−13.20	0.29	4	8
N I	8686.15	10.33	−0.305	−30.07	−13.20	0.29	4	8
Fe I	8688.63	2.17	−1.212	−30.48	−13.78	0.29		
S I	8693.24	7.87	−1.380	−28.98	−11.93	0.29		
S I	8693.98	7.87	−0.520	−28.98	−11.93	0.29		
S I	8694.70	7.87	+0.050	−28.98	−11.93	0.29		
Fe I	8699.45	4.96	−0.380	−29.34	−12.40	0.29		
N I	8703.25	10.33	−0.322	−30.07	−13.21	0.29	4	8
Fe I	8710.39	4.91	−0.646	−29.39	−12.45	0.29		
N I	8711.70	10.33	−0.234	−30.07	−13.21	0.29	4	8
Mg I	8717.83	5.93	−0.930	−27.61	−10.16	0.29		
N I	8718.84	10.34	−0.335	−30.07	−13.20	0.29	4	8
Fe II	8722.35	9.85	−0.383	−30.02	−12.62	0.29		
Fe II	8722.46	12.17	+0.862	−30.07	−11.77	0.29		
Si I	8728.01	6.18	−0.610	−28.31	−11.04	0.29		
N I	8728.90	10.33	−1.065	−30.08	−13.21	0.29	4	8
Mg I	8736.02	5.95	−0.690	−27.58	−10.07	0.29		
Mg I	8736.03	5.95	−1.020	−27.58	−10.07	0.29		
Si I	8742.45	5.87	−0.630	−28.86	−11.65	0.29		
Mg II	8745.66	12.09	−0.380	−28.63	−11.06	0.29		
N I	8747.37	10.34	−1.320	−30.07	−13.20	0.29	4	8
H I	8750.47							
Si I	8752.00	5.87	−0.520	−28.86	−11.66	0.29		

Table 3. Stellar parameters and derived abundances for our program stars.

HD	$b-y$ [mag]	m_1 [mag]	c_1 [mag]	β [mag]	$T_{\rm eff}$ [K]	$\log g$ [dex]	$v \sin i$ [km s^{-1}]	[N] LTE	[N] NLTE	[S] LTE	[S] NLTE	[Ca] LTE
31295	0.044	0.178	1.007	2.898	9100	4.1	120[1]	−0.20	−0.45	+0.00	−0.14	−0.70
64491	0.196	0.132	0.669	2.734	7100	4.1	170[2]	−0.15	−0.30	+0.00	−0.09	−0.95
75654	0.161	0.140	0.816	2.753	7200	3.8	65[2]	+0.65	+0.30	+0.00	−0.10	−1.00
91130	0.073	0.158	1.035	2.854	8000	3.8	135[1]	−0.05	−0.30	+0.30	+0.18	−3.00
111005	0.223	0.135	0.698		7400	3.8	140[2]					−0.40
120500	0.068	0.170	1.062	2.871	8200	3.9	125[1]	−0.05	−0.30	+0.00	−0.13	−0.30
125162	0.051	0.182	1.000	2.894	8900	4.1	128[1]	−0.30	−0.50	−0.30	−0.45	−2.00
141851	0.071	0.165	1.001	2.846	8100	3.8	280[1]					−1.30
142703	0.180	0.118	0.725	2.743	7200	4.0	100[1]	−0.50	−0.60	−0.50	−0.53	−1.40
148638	0.129	0.155	1.085	2.818	7800	3.4	160[2]	+0.40	+0.05	+0.40	+0.21	−1.20
149303	0.064	0.180	1.028	2.848	8000	3.8	275[1]					−0.50
183324	0.051	0.165	1.003	2.890	9300	4.1	90[3]	+0.00	−0.30	+0.00	−0.13	−1.40
192640	0.101	0.157	0.927	2.833	8000	3.9	80[1]	−0.40	−0.55	−0.30	−0.39	−1.50
193281	0.098	0.152	1.109	2.844	8100	3.6	95[1]	+0.30	−0.05	+0.30	+0.14	−1.50
204041	0.093	0.167	0.940	2.845	8100	4.0	65[3]	−0.15	−0.35	−0.05	−0.17	−0.70
221756	0.056	0.166	1.072	2.878	8800	3.8	112[1]	−0.25	−0.50	+0.20	+0.06	−0.40

[1] Paunzen et al. (1999b); [2] derived from the Paschen lines in our spectra; [3] Holweger & Rentzsch-Holm (1995).

Additional observations were performed in May 1998 at the Complejo Astronómico el Leoncito (CASLEO) using the 2.15 m telescope equipped with a REOSC echelle spectrograph[1] and a Tek-1024 CCD. A grating with 79 lines mm^{-1} was used as a cross disperser yielding a resolving power of about 28 000.

All frames have been bias-subtracted, flat-fielded and wavelength calibrated using standard IRAF procedures. The spectral region of sulphur and nitrogen lines around 8670 Å has the advantage of being free of telluric lines. Well-known heavy fringing in the near-IR was the gravest problem we met. Additional observations of fast-rotating hot stars in the same spectral region have been carried out to facilitate finding of the optimal flat-fielding recipe, thus minimizing the amplitudes of the residual fringes. The typical signal-to-noise ratio for most of the spectra is between 100 and 200.

Our spectra indicate that HD 64491 is a previously undetected spectroscopic binary system with a high and a low $v \sin i$ component. On top of the extremely broad stellar lines of the primary fitted in this paper ($v \sin i$ = 170 km s^{-1}), we find a much narrower component of the secondary. This holds not only for the strong Paschen line, but also for the less pronounced metal lines.

We note that there are still fringes present in the spectra taken at CASLEO (Figs. 1 and 2). However, we are confident that these fringes do not affect the relevant regions in our spectra.

[1] On loan from the Institute Astrophysique de Liège, Belgium.

3. Model atmospheres and spectrum synthesis

For all stars except one, namely HD 64491, we already calculated model atmospheres in Paper I, based on Kurucz's ATLAS9 code (Kurucz 1993). For HD 64491 we now proceed in exactly the same way and derive the following atmospheric parameters: $T_{\rm eff}$ = 7100 K, $\log g$ = 4.1 dex. All stellar parameters are summarized in Table 3 and the typical errors are ±200 K for the effective temperature and ±0.2 dex for the gravity (see Paper I). The microturbulence is 3 km s^{-1} for all program stars.

We included the latest published VCS Stark broadening tables for hydrogen (Lemke 1997) in the spectrum sythesis code LINFOR (for a more detailed discussion see Rentzsch-Holm 1997) and in the Kiel NLTE code to account for hydrogen background lines. The latter will be discussed in more detail in Sect. 3.1.

Due to the presence of the Paschen lines, the normalisation of the spectra is not straightforward. In order to make the normalisation procedure as objective as possible, we define a priori a sample of wavelengths at which the local continuum – given by the Paschen lines – is reached; there are no spectral lines other than the Paschen lines at these wavelengths. We calculate then a synthetic spectrum for each star including the Paschen lines and solar abundances. The normalisation is done by dividing the observed spectrum by the synthetic one and using a least square fit to determine the normalisation curve. This curve turns out in all cases to be a smooth function of wavelength. Division of the observed spectrum and this normalisation curve gives the normalised spectrum.

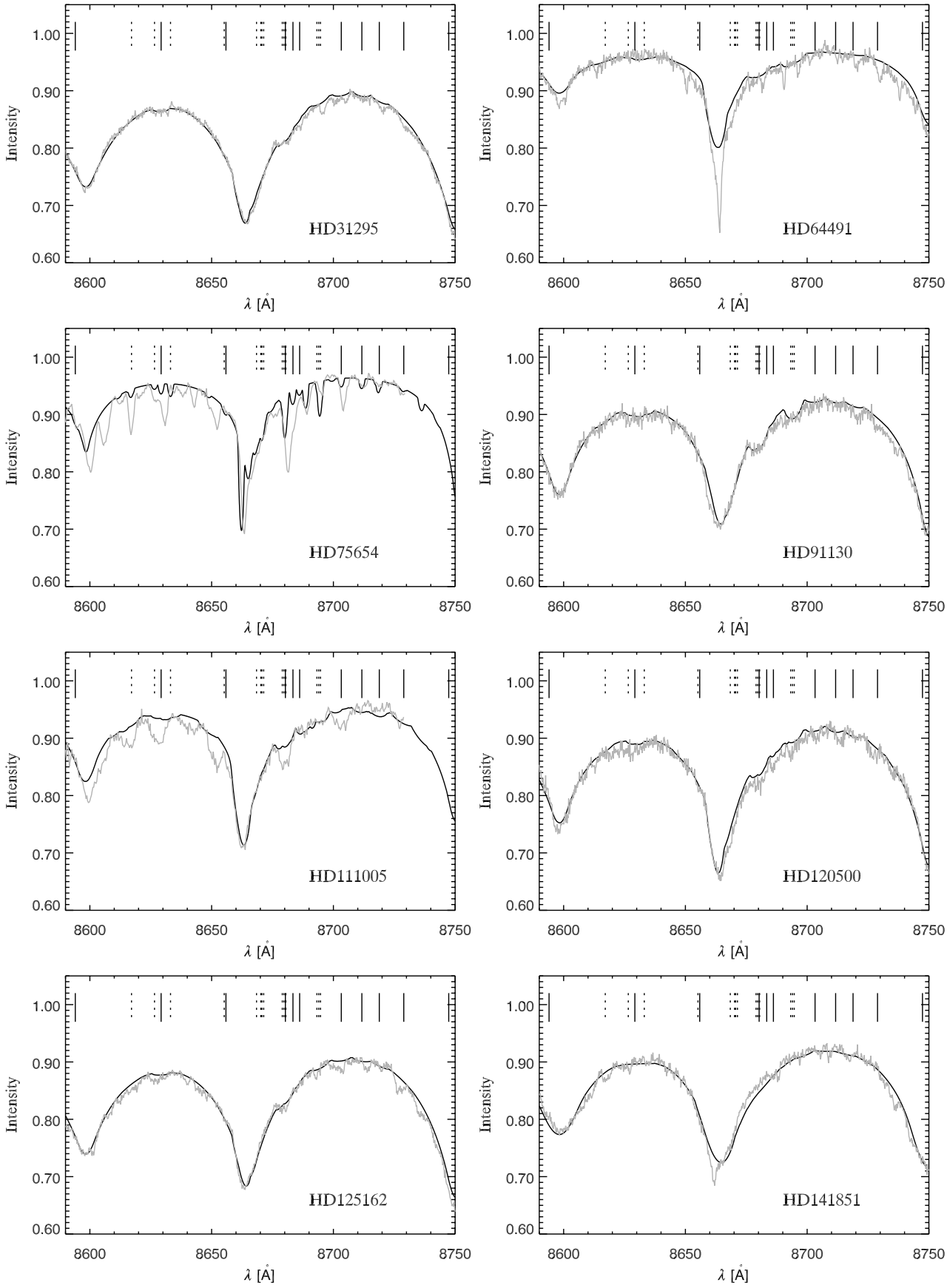

Fig. 1. Observed (solid grey line) and synthetic spectrum (solid black line) for the program stars HD 31295, HD 64491, HD 75654, HD 91130, HD 111005, HD 120500, HD 125162, HD 141851. The position of the N and S lines are overplotted by solid and dotted lines respectively. In HD 75654 and HD 111005 the remaining fringes are very strong. HD 64491 is a spectroscopic binary.

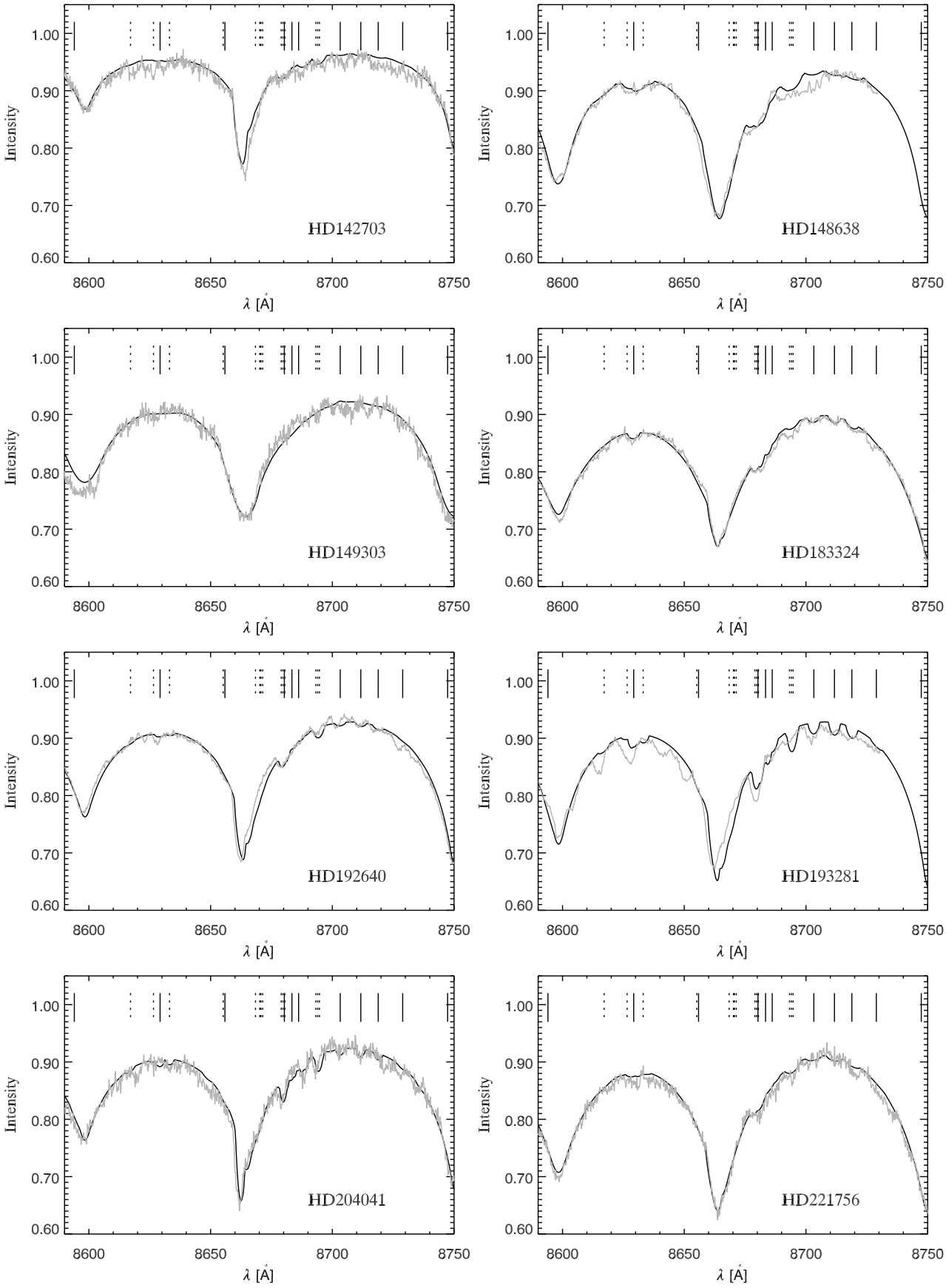

Fig. 2. Observed (solid grey line) and synthetic spectrum (solid black line) for the program stars HD 142703, HD 148638, HD 149303, HD 183324, HD 192640, HD 193281, HD 204041, HD 221756. The position of the N and S lines are overplotted by solid and dotted lines respectively. In HD 193281 the remaining fringes are very strong while HD 142703 and HD 148638 show some minor remaining features around 8700 Å.

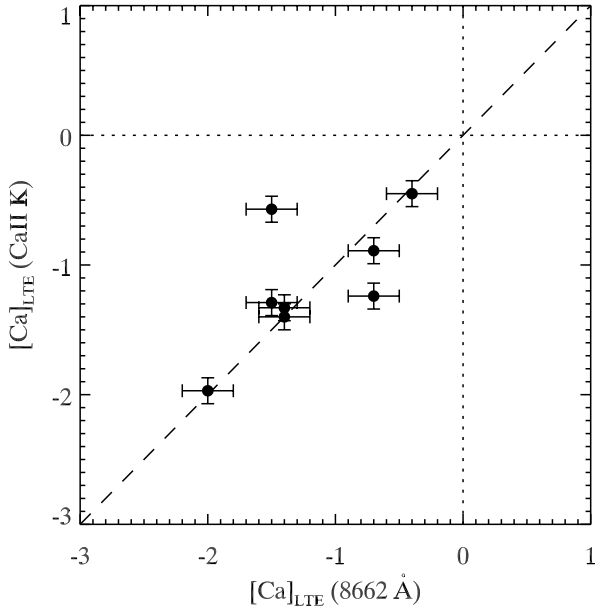

Fig. 3. Calcium abundance from the Ca II K line (Holweger & Rentzsch-Holm 1995; Holweger et al. 1999) versus the calcium abundance from the 8662 Å line (this work) in the program stars.

3.1. The nitrogen model atom

We use the nitrogen model atom of Rentzsch-Holm (1996) and take into account the results of Lemke & Venn (1996). They find that the statistical equilibrium of nitrogen is almost completely controlled by the UV flux at the N I resonance line at 1199 Å. The flux in this wavelength region is very sensitive to the carbon abundance, because of the C I ionisation edge at 1100 Å, and to the shape of the Lyman α line. Following the same approach as Lemke & Venn (1996) we included the Lyman α line explicitly in the NLTE calculations.

It turns out that, if we include Lyman α in the calculation of the line rates, the general metallicity of the atmosphere has only a minor effect (see also Fig. 2 of Lemke & Venn 1996). Moreover, we show in Paper I that the carbon abundance is on the average solar in the λ Bootis stars. Hence we carry out all NLTE calculations accounting for the Lyman α background line and using solar ODF's and stellar atmospheres of solar metallicity.

3.2. The non-LTE abundance corrections for the Si lines

For the sulphur lines in our list we use the non-LTE abundance corrections calculated by Takada-Hidai & Takeda (1996). They tabulate them for each line as a function of effective temperature for a constant $\log g$ of 4.0 dex and a microturbulence of $\zeta = 2$ km s^{-1}. Since the corrections depend only weakly on $\log g$ and ζ, we can use this table for our whole sample of stars. The abundance corrections are always negative and lie for our stars typically between -0.1 and -0.2 dex.

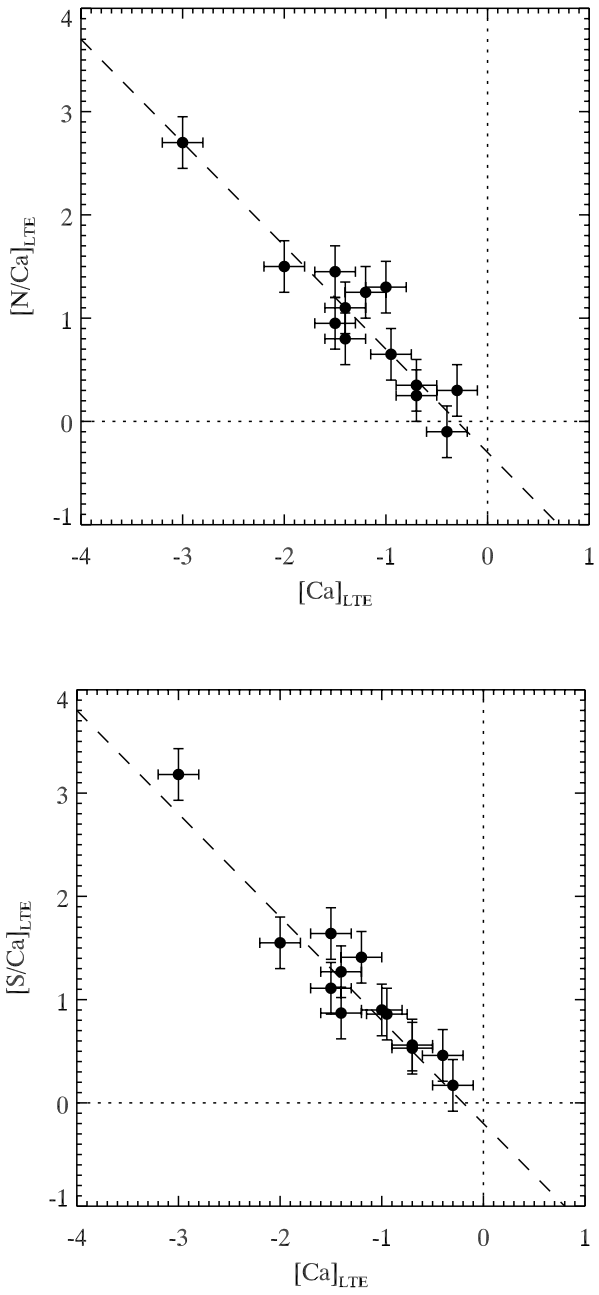

Fig. 4. [N/Ca] and [S/Ca] versus [Ca] abundance (taken from Table 3) in the program stars.

3.3. The line data

Table 2 summarizes the line data for the spectrum synthesis interval from 8590 to 8755 Å. A check of the VALD database, using our range of stellar parameters, reveals, that we need the following ions: H I, N I, S I, Mg I, Mg II, Al II, Si I, Ca II, Fe I, and Fe II. The data for the respective lines is taken from Wiese et al. (1966, 1996), and from the VALD database (Kupka et al. 1999; Ryabchikova et al. 1999; Piskunov et al. 1995). Additional information for the calculation of the line broadening parameters, as for example the azimuthal quantum number or the configuration of the parent state, is found in Moore (1971).

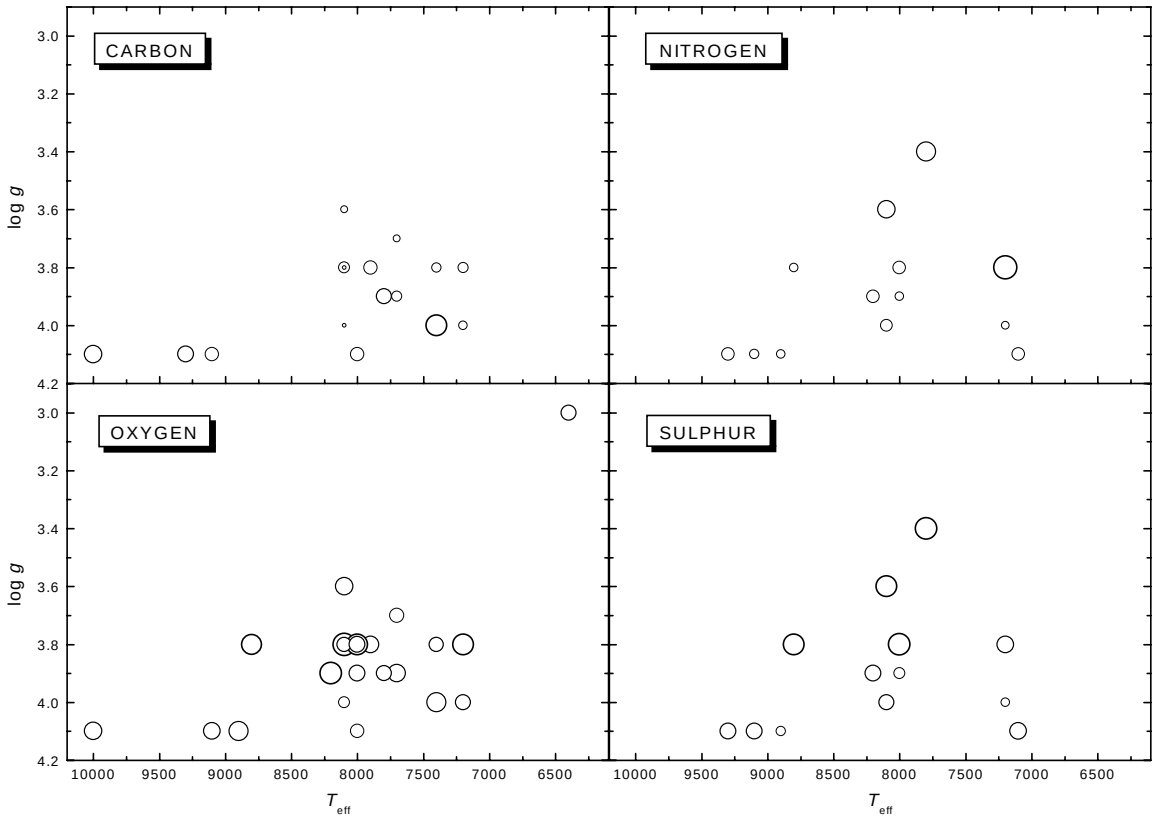

Fig. 5. Surface gravity versus effective temperature for all programs stars of Paper I and this work. The size of the circles in each diagram shows the abundance of the respective element; small circles denote underabundances.

4. Abundances

The abundance determination proceeds in two steps: we derive $v \sin i$ (if unknown) and the calcium abundance from the Ca/H blend at 8662 Å. If no a priori abundance value for the above mentioned relevant metals (Fe, Al, Mg and Si) was found in the literature, we fix their abundance by using the value of Ca. This has little influence on the N and S abundance, because the blends are usually extremely weak. Finally we determine the abundances of the two light elements N and S.

The abundances for our program stars are depicted in Table 3. The typical errors from the spectrum synthesis are slightly larger than in Paper I due to the problems with continuum placement. Especially for the weak N and S lines on top of the Paschen wings we derive a typical error of ±0.2 dex from spectrum synthesis. For the fast rotators this error is even larger because the line depth becomes even smaller and the lines more difficult to define against the local continuum. The typical error for calcium is much smaller, ±0.1 dex, because the blend with the hydrogen line is very strong and can be nicely fitted using the VCS tables of Lemke (1997). For the three stars HD 111005, HD 141851, and HD 149303 the residual fringes are too strong to derive reliable N and S abundances. Figures 1 and 2 illustrate the observed and fitted spectra for all our program stars and give an impression of the quality of the fits.

The mean NLTE nitrogen abundance of the program stars is −0.30 dex with respect to the Sun; hence it follows the general trend of carbon, which is also slightly underabundant in λ Bootis stars, −0.37 dex (Paper I). The mean sulphur abundance on the other hand is slightly larger −0.11 dex. Nevertheless, the calcium abundances are typically much smaller and reveal a much larger star-to-star scatter than the light element abundances.

We find a good correlation between the calcium abundance derived from the Ca II K line (Holweger & Rentzsch-Holm 1995; Holweger et al. 1999) and the Ca abundance derived in this work from the 8662 Å line (Fig. 3).

Up to now N and S abundances for λ Bootis stars are scarce in the literature and a detailed comparison as it is done for calcium is generally not possible (Table 4).

5. Discussion

For the first time, we have derived a complete set of light element abundances (C, N, O and S) for a homogeneous sample of λ Bootis stars. The sample spans the whole range of effective temperatures, surface gravities and projected rotational velocities known for these stars. Despite the fact that the near infrared presents a wealth of N and S lines, these become extremely difficult to analyze for $v \sin i$ larger than 100 km s^{-1}. The results of Paper I and this work are summarized in Table 5. Similar to the

Table 4. Nitrogen, sulphur and calcium abundances from the literature of well-established λ Bootis stars; all results are based on LTE analysis of spectra in the optical region. The calcium data is from the Ca II K line (Holweger & Rentzsch-Holm 1995; Holweger et al. 1999).

HD	HR	[N] [dex]	[S] [dex]	Ref.	[Ca] [dex]
15165			+0.00	2	
31295	1570	−0.02	+0.00	1	−0.89
			−0.40	4	
84123		+0.00	−0.50	3	
101108		<+0.70		5	
107233		<+0.20		5	
125162	5351	+0.06		1	−1.97
142703			<−0.70	5	−1.33
183324	7400	−0.10	<+0.30	3	−1.40
192640	7736	−0.14	−0.23	1	−1.29
		<+0.30	<−0.20	4	
193281	7764A				−0.57
204041	8203		+0.40	4	−1.24
221756	8947				−0.45

1: Venn & Lambert (1990); 2: Chernyshova et al. (1998); 3: Heiter et al. (1998); 4: Paunzen et al. (1999a); 5: Heiter (2001).

Table 5. Non-LTE abundances for C, N, O and S of all program stars from Paper I and this work; the typical errors are 0.2 dex.

HD	[C] [dex]	[N] [dex]	[O] [dex]	[S] [dex]
319	−0.36		+0.22	
4158			−0.16	
6870	+0.14		+0.05	
11413	−0.25		−0.10	
30422	−0.27		−0.25	
31295	−0.25	−0.45	−0.08	−0.14
64491		−0.30		−0.09
75654	−0.44	+0.30	+0.14	−0.10
91130		−0.30	+0.14	+0.18
120500		−0.30	+0.19	−0.13
125162		−0.50	+0.02	−0.45
141851	−0.81		−0.21	
142703	−0.52	−0.60	−0.19	−0.52
148638		+0.05		+0.21
149303			−0.14	
168740	−0.42		−0.03	
170680	−0.06		−0.07	
183324	−0.14	−0.30		−0.13
192640		−0.55	−0.15	−0.39
193256	−0.62		−0.23	
193281	−0.61	−0.05	−0.05	+0.14
198160/1	−0.16		−0.18	
204041	−0.81	−0.35	−0.38	−0.17
210111	−0.45		−0.20	
221756		−0.50	+0.10	+0.15

other light elements carbon and oxygen, we find an anti-correlation between the nitrogen/sulphur abundance and the calcium abundance (Fig. 4). For a comparison with other work, especially comparing these light element abundances to other metal abundances, one has to account for systematic effects that may arise from using different stellar parameters for the same star. This once again stresses the importance of a homogeneous analysis as it is carried out in these two papers (Table 5).

We conclude three main points from this analysis:

- The star-to-star scatter in the light element abundances C, N, O and S is much smaller than in the respective metal abundances like Ca;
- The abundances of C, N, O and S are not strictly solar, but range instead from −0.8 dex to +0.2 dex;
- The metal abundances show typically a significant offset with respect to the light elements, Fe-peak elements being always more underabundant.

From our analysis we can therefore conclude that the λ Bootis stars are Population I stars, hence their large metal underabundances are indeed a surface phenomenon. Figure 5 reveals that there is no clear correlation between the light element abundances and the stellar parameters $T_{\rm eff}$ and $\log g$. Futhermore we do not detect any correlation between the abundances and $v \sin i$ nor among the abundances of C, N, O, and S themselves. Reading Fig. 5 as a Hertzsprung-Russell-diagram, it reveals no clear correlation between the abundance pattern of a star and its evolutionary state.

Considering now the possible scenarios (Sect. 1) proposed to explain the λ Bootis stars, we comment in the following on some of them.

Andrievsky (1997) concluded that according to his scenario the N/C ratio in some λ Bootis stars should be larger than solar. Of the six stars for which we have C and N abundances, three show an N/C ratio larger than solar (HD 31295, HD 142703, and HD 183324).

The theoretical work of Charbonneau (1993) and Turcotte & Charbonneau (1993) is unfortunately restricted to the two elements calcium and titanium, so that we cannot draw any conclusions regarding our light element abundances.

The anticorrelations between the light elements and calcium/silicon are in agreement with the accretion of metal-poor gas onto the star.

Acknowledgements. The authors acknowledge the use of the CCD and data acquisition system supported by US NSF Grant AST 90-15827 (R.M. Rich). Inga Kamp acknowledges support by the "Deutsche Forschungsgesellschaft" under grant Ho 596/35-2 and by a Marie Curie Fellowship of the European Community programme "Improving Human Potential" under contract number MCFI-1999-00734. This research has made use of the VALD database and of the SIMBAD database, operated at CDS, Strasbourg, France.

References

Andrievsky, S. M. 1997, A&A, 321, 838
Aumann, H. H., Gillett, F. C., Beichmann, C. A., et al. 1984, ApJ, 278, L23
Charbonneau, P. 1991, ApJ, 372, L33
Charbonneau, P. 1993, ApJ, 405, 720
Cheng, K. P., Bruhweiler, F. C., Kondo, Y., & Grady, C. A. 1992, ApJ, 396, L83
Chernyshova, I. V., Andrievsky, S. M., Kovtyukh, V. V., & Mkrtichian, D. E. 1998, Contributions of the Astronomical Observatory Skalnaté Pleso, 27(3), 332
Cowley, C. R. 1971, Observatory, 91, 139
Faraggina, R., & Bonifacio, P. 1999, A&A, 349, 521
Gerbaldi, M. 1991, in The Infrared Spectral Region of Stars, ed C. Jaschek, & Y. Andrillat (Cambridge University Press, Cambridge), 307
Gillett, F. C. 1986, in Light on Dark Matter, ed F. Israel (Dordrecht, D. Reidel Publishing Co.), 61
Gray, R. O., & Corbally, C. J. 1993, AJ, 106, 632
Gray, R. O., & Corbally, C. J. 1997, BAAS, 29(5), 1286
Griem, H. R. 1968, Phys. Rev., 165, 258
Heiter, U. 2000, PASP, 112, 1509
Heiter, U. 2001, A&A, submitted
Heiter, U., Kupka, F., Paunzen, E., Weiss, W. W., & Gelbmann, M. 1998, A&A, 335, 1009
Holweger, H., & Stürenburg, S. 1993, PASPC, 44, 356
Holweger, H., & Rentzsch-Holm, I. 1995, A&A, 303, 819
Holweger, H., Hempel, M., & Kamp, I. 1999, A&A, 350, 603
Kupka, F., Piskunov, N. E., Ryabchikova, T. A., Stempels, H. C., & Weiss, W. W. 1999, A&A, 138, 119
Kurucz, R. L. 1993, CD-ROM 1-23, Smithsonian Astrophysical Observatory
Lemke, M. 1997, A&AS, 122, 285
Lemke, M., & Venn, K. A. 1996, A&A, 309, 558
Michaud, G., & Charland, Y. 1986, ApJ, 311, 326
Moore, C. E. 1971, Atomic energy levels, National Bureau of Standards, Reference Series, vols. I−III
Oudmaijer, R. D., van der Veen, W. E. C. J., Waters, L. B. F. M., et al. 1992, A&AS, 96, 625
Paunzen, E. 1997, A&A, 326, L29
Paunzen, E., Andrievsky, S. M., Chernyshova, I. V., et al. 1999a, A&A, 351, 981
Paunzen, E., Kamp, I., Iliev, I. Kh., et al. 1999b, A&A, 345, 597, Paper I
Piskunov, N. E., Kupka, F., Ryabchikova, T. A., Weiss, W. W., & Jeffery, C. S. 1995, A&AS, 112, 525
Rentzsch-Holm, I. 1996, A&A, 305, 275
Rentzsch-Holm, I. 1997, A&A, 317, 178
Ryabchikova, T. A., Piskunov, N. E., Stempels, H. C., Kupka, F., & Weiss, W. W. 1999, Phys. Scr. T, 83, 162
Sadakane, K., & Nishida, M. 1986, PASP, 98, 685
Takada-Hidai, M., & Takeda, Y. 1996, PASJ, 48, 739
Turcotte, S., & Charbonneau, P. 1993, ApJ, 413, 376
Unsöld, A. 1968, Physik der Sternatmosphären, 2. Aufl. (Springer Verlag, Heidelberg)
Venn, K. A., & Lambert, D. L. 1990, ApJ, 363, 234
Waters, L. B. F. M., Trams, N. R., & Waelkens, C. 1992, A&A, 262, L37
Wiese, W. L., Smith, M. W., & Glennon, B. M. 1966, Atomic Transition Probabilities vol. I, Nat. Stand. Ref. Data Ser., Nat. Bur. Stand. (U.S.)
Wiese, W. L., Fuhr, J. R., & Deters, T. M. 1996, Journal of Physics and Chemical Reference Data, Monograph No. 7: Atomic Transition Probabilities of Carbon, Nitrogen, and Oxygen